

Simulation & Evaluation of (OADM) Based on Bragg Gratings and 3dB MMI Couplers

Dr. Aied K. Mohammed

Electrical Engineering Department, University of Technology / Baghdad.

Raheel J. Hassoon

Electrical Engineering Department, University of Technology / Baghdad.

Email:alsamarrie@yahoo.com

Received on:26/3/2014 & Accepted on:1/8/2015

ABSTRACT

In this paper, an approach has been proposed to design an (OADM) made in silica- on silicon waveguide by combining Bragg gratings (BGs) and 2x2 3dB multimode interference couplers (3dB MMI coupler) in a Mach-Zehnder interferometer. This design technique shows an interesting result in obtaining low insertion loss, low return loss, insensitive to polarization, high thermal stability, large optical bandwidth and low crosstalk.

Key word: Optical add/drop multiplexer (OADM), Bragg grating (BG), Mach-Zehnder Interferometer (MZI), Multimode interference couplers (MMI coupler).

محاكاة وتقييم لـ(OADM)المبني على اساس محززات براغ ووصلات التداخل المتعدد
(3 دسيبل)

الخلاصة :

في هذا البحث تم عمل تصميم جديد لـ(OADM) من مادة السلكا فوق دليل موجي من السلكون من خلال الجمع بين محززات الحيود لبراغ (BG) ووصلات التداخل المتعدد من نوع (2x2 3dB MMI coupler) في تداخل ماخ زيندر . يظهر هذا التصميم نتيجة مثيرة للاهتمام من خلال الحصول على فقدان إدراج منخفض ، وانخفاض خسارة العودة، وعدم التأثير بالاستقطاب وله استقرارية حرارية عالية، وعرض نطاق ترددي ضوئي كبير وكذلك قليل في انتقال المعلومات من قناة الى اخرى .

INTRODUCTION

The fiber band-pass filters based on the Michelson (MI) / Mach-Zehnder (MZI) interferometers is usually fabricated from a pair of Bragg grating (BG), matched reflection gratings play an important role in optical fiber communication systems. Simulation and experimental results show that the MZI with BG filters can have low loss,

very spectrally selective, and low cost. The MZI with BG and 3dB multimode interference (MMI) couplers has a high-performance in a dense wavelength-division multiplexer/demultiplexer applications [1, 2]. The MMI couplers have many advantages such as, small size, insensitive to polarization, insensitivity to fabrication errors, compact construction, simple fabrication techniques, high thermal stability, large optical bandwidth and low crosstalk [3, 4, 5, 6]. A Bragg grating is made of a small section of fiber cable, which is modified by exposure to ultraviolet radiation to create periodic changes in the refractive index of the fiber core. The Bragg grating reflects some of the light waves when travelling through it. The reflected waves usually occur at one particular wavelength, and the reflected wavelength is known as the Bragg resonance wavelength. The Bragg resonance wavelength depends on the change of the refractive index that is applied to the Bragg grating. In addition, the wavelength of the reflected wave also depends on the basic parameters of the grating (the grating period, the grating length, and the modulation depth) [7]. There are many advantages of fiber gratings over competing technologies such as, low insertion loss (around 0.1dB), high return loss, ease of coupling with other fibers, polarization insensitivity, low temperature coefficient less than (0.7 pm/C°) and low cost. One of the most distinguishing features of gratings techniques is the flexibility which can be used to achieve a desired spectral characterization. Many physical parameters of the grating can be varied, including: induced index change, length, apodization, period chirp, fringe tilt, and whether the grating supports counter propagating or copropagating coupling at a desired wavelength. By varying these parameters, gratings can be made with normalized bandwidths $(\Delta\lambda/\lambda)$ between (0.1) to (10^{-4}) [8].

The proposed system involves design, the (OADM) which consists of three stages: the first one is to design and simulate 2X2 3dB MMI coupler by using (OptiBPM 9) software. The second stage is to design and simulate the Bragg Grating (BG) by using the (OptiGrating 4.2) software, it provides an accurate analysis of the BG characteristics. The third stage is to design and simulate a proposed OADM by combining the previous stages to study the performance of each port of the OADM. A software package (OptiSystem 11) is used for this purpose, this software is used to obtain the eye diagrams, estimate the Q-factor and the BER for the proposed OADM in DWDM system. The (OADM) was simulated to add and drop with channel wavelength = 1550 NM at transmission data rate of 10 GB/s. The DWDM system which was used in the simulation has 16 channels, the channel spacing was equal to 100 GHz (0.8 nm), the power of each channel was assumed to be 1mW (0 dBm) and the modulator was NRZ-OOK. The simulation results give insertion loss equal to 0.6 dB, polarization dependent loss (PDL) equal to 0.00446 dB, the crosstalk due to adjacent channels (interband crosstalk) was less than -28 dB, non-adjacent channel isolation is more than 55 dB, interband crosstalk is less than -49 dB, return loss is less than -55 dB and the Q-factor is 62.

The analysis results show that using 3dB MMI coupler techniques give advantage, this analysis shows that an improvement of the insertion loss by 1.4 dB was achieved. In addition the crosstalk is improved by -19 dB for the 1550 nm dropping signal. It has the advantages in downsizing and cost-effectiveness compared with the circulator techniques.

A single Bragg grating in a single-mode fiber acts as a wavelength-selective distributed reflector or a band rejection filter by reflecting wavelengths around the Bragg resonance. However, placing identical gratings in two arms of a MZI can make a band pass filter. Fig. (1) Shows the proposed technique in this paper.

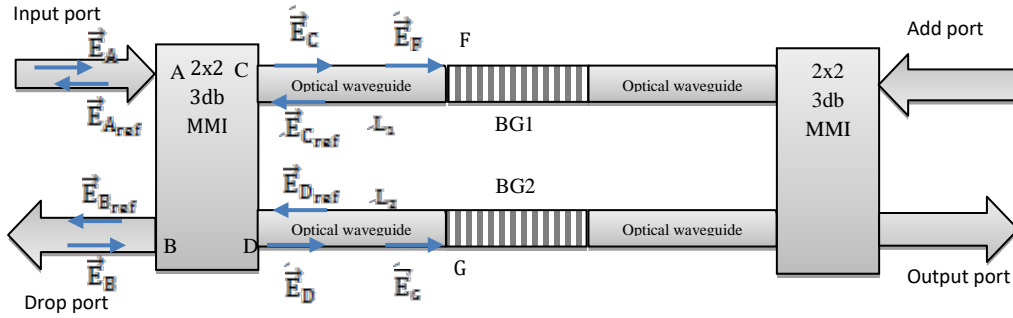


Figure (1). The proposed technique

According to Figure (1) if the power splitting ratio of the MMI coupler is (α) the optical field transfer matrix is [9, 10]:

$$\begin{bmatrix} \vec{E}_C \\ \vec{E}_D \end{bmatrix} = \begin{bmatrix} \sqrt{1-\alpha} & j\sqrt{\alpha} \\ j\sqrt{\alpha} & \sqrt{1-\alpha} \end{bmatrix} \begin{bmatrix} \vec{E}_A \\ \vec{E}_B \end{bmatrix} \quad (1)$$

Optic fields are generally vectorial and their polarization states may change along the optical waveguide arm because of the birefringence. Due to the effects of optical waveguide propagation delays in the two arms and their polarization rotation, the relationship between fields (\vec{E}_F, \vec{E}_G) and input fields (\vec{E}_C, \vec{E}_D) can be expressed in a transfer matrix as;

$$\begin{bmatrix} \vec{E}_F \\ \vec{E}_G \end{bmatrix} = \begin{bmatrix} [U''] \exp(-j\theta_1 - j\varphi_1) & 0 \\ 0 & [V''] \exp(-j\theta_2 - j\varphi_2) \end{bmatrix} \begin{bmatrix} \vec{E}_C \\ \vec{E}_D \end{bmatrix} \quad (2)$$

Where

$(\theta_1 = \frac{2\pi n_r}{\lambda} L_1)$ and $(\theta_2 = \frac{2\pi n_r}{\lambda} L_2)$ are the phase delays of the two fiber arms, (n_r) is the core reflect index, (φ_1) and (φ_2) are the initial optical phases, and (U'') and (V'')

represents the birefringence effect in the two arms, ($//$) is the parallel polarization of forward propagated optical signal. In each arm, the Bragg grating (BG) with reflectivities of (R_1) and (R_2), reflects the optical signal and also rotates its polarization state by (90°). The backward propagating optical field will have vertical (\perp) polarization with respect to the forward propagating signal. The transfer matrix of the backward propagated optical fields is:

$$\begin{bmatrix} \vec{E}_{C_{ref}} \\ \vec{E}_{D_{ref}} \end{bmatrix} = \begin{bmatrix} [U^\perp]R_1 \exp(-j\theta_1 - j\varphi_1) & 0 \\ 0 & [V^\perp]R_2 \exp(-j\theta_2 - j\varphi_2) \end{bmatrix} \begin{bmatrix} \vec{E}_F \\ \vec{E}_G \end{bmatrix} \quad (3)$$

where U^\perp and V^\perp represent the birefringence effect in the two optical waveguide arms. Substituting \vec{E}_F and \vec{E}_G from Eq. (2) in Eq. (3), the relationship between reflected fields ($\vec{E}_{C_{ref}}$, $\vec{E}_{D_{ref}}$) and transmitted fields (\vec{E}_C , \vec{E}_D) the transmission matrix can be written as;

$$\begin{bmatrix} \vec{E}_{C_{ref}} \\ \vec{E}_{D_{ref}} \end{bmatrix} = \begin{bmatrix} [U//U^\perp]R_1 \exp(-j2\theta_1 - j\varphi_1) & 0 \\ 0 & [V//V^\perp]R_2 \exp(-j2\theta_2 - j\varphi_2) \end{bmatrix} \begin{bmatrix} \vec{E}_C \\ \vec{E}_D \end{bmatrix} \quad (4)$$

Because of the exchange principle, both $[U//U^\perp]$ and $[V//V^\perp]$ will be independent of the actual birefringence of the optical waveguide. Therefore, in the following analysis, the polarization effect is neglected and $[U//U^\perp]=[V//V^\perp]=1$ will be assumed. The backward propagated optical fields passing through the same fiber directional coupler are:

$$\begin{bmatrix} \vec{E}_{A_{ref}} \\ \vec{E}_{B_{ref}} \end{bmatrix} = \begin{bmatrix} \sqrt{1-\alpha} & j\sqrt{\alpha} \\ j\sqrt{\alpha} & \sqrt{1-\alpha} \end{bmatrix} \begin{bmatrix} \vec{E}_{C_{ref}} \\ \vec{E}_{D_{ref}} \end{bmatrix} \quad (5)$$

($\vec{E}_{C_{ref}}$, $\vec{E}_{D_{ref}}$) from Eq.(4) is substituted in the Eq. (5) and (\vec{E}_C , \vec{E}_D) from Eq. (1) is substituted with $\begin{bmatrix} \sqrt{1-\alpha} & j\sqrt{\alpha} \\ j\sqrt{\alpha} & \sqrt{1-\alpha} \end{bmatrix} \begin{bmatrix} \vec{E}_A \\ \vec{E}_B \end{bmatrix}$ therefore, the overall transfer matrix is from the input (\vec{E}_A , \vec{E}_B) to the output ($\vec{E}_{A_{ref}}$, $\vec{E}_{B_{ref}}$) is:

$$\begin{bmatrix} \vec{E}_{A_{ref}} \\ \vec{E}_{B_{ref}} \end{bmatrix} = \begin{bmatrix} \sqrt{1-\alpha} & j\sqrt{\alpha} \\ j\sqrt{\alpha} & \sqrt{1-\alpha} \end{bmatrix} \begin{bmatrix} R_1 \exp(-j2\theta_1 - j\varphi_1) & 0 \\ 0 & R_2 \exp(-j2\theta_2 - j\varphi_2) \end{bmatrix} \begin{bmatrix} \sqrt{1-\alpha} & j\sqrt{\alpha} \\ j\sqrt{\alpha} & \sqrt{1-\alpha} \end{bmatrix} \begin{bmatrix} \vec{E}_A \\ \vec{E}_B \end{bmatrix} \quad (6)$$

For unidirectional application, this fiber Michelson interferometer can be used as an optical filter. Let ($\vec{E}_B = 0$), the filter transfer function can be given as [25, 26]:

$$P_T = \left| \frac{\vec{E}_{B_{ref}}}{\vec{E}_A} \right|^2 = \alpha (1-\alpha) |R_1 \exp(-j2\theta_1 - j\varphi_1) + R_2 \exp(-j2\theta_2 - j\varphi_2)|^2$$

$$= \alpha (1-\alpha) \{R_1^2 + R_2^2 + 2R_1R_2(\cos(2\Delta\theta + 2\Delta\varphi))\} \quad (7)$$

$$P_{ref} = \left| \frac{\vec{E}_{A_{ref}}}{\vec{E}_A} \right|^2 = \alpha (1-\alpha) \{R_1^2 + R_2^2 - 2R_1R_2(\cos(2\Delta\theta + 2\Delta\varphi))\} \quad (8)$$

Where

($\Delta\theta = \theta_1 - \theta_2 = \left(\frac{2\pi n_g}{\lambda}\right) \Delta L$), is the differential phase delay and ($\Delta\varphi = (\varphi_1 - \varphi_2)/2$) is the initial phase difference between the two arms. In case the Bragg grating (BG) has the same reflectivity ($R_1 = R_2 = R$), neglecting the propagation loss of the optical waveguide arms, the initial phase difference between the two arms equal to zero and the optical path length difference between arms equal to zero ($\Delta L = L_1 - L_2 = 0$) or an integer number of half-wavelengths. The Eq. (7,8) can be written as;

$$P_T = 4 \alpha (1-\alpha) R^2 \quad (9)$$

$$\text{And } P_{ref} = \alpha (1-\alpha) \{R_1^2 + R_2^2 - 2R_1R_2\} = 0 \quad (10)$$

Eq. (9,10) is equivalent to an ideal dual grating Mach-Zehnder interferometer (DGMZI-OADM).

Design of the 3dB MMI Coupler:

To build a 2x2 3dB MMI coupler in which the phase difference between the outputs is ($\pi/2$), the MMI device must be based on an even (General Multimode Interference) coupler and the length of the 3dB coupler is $1.5 * L_\pi$. The L_π is defined as the beat length (or coupling length).

In the General Multimode Interference (GMMI), length of the 3dB coupler is defined as:

$$L_{MMI} = \frac{M}{N} 3L_\pi \quad (11)$$

Where

N is the number of self-images. M is an integer without a common divisor with N that defines the several possible device lengths. In this case $M = 1$ and $N = 2$.

$$L_{\pi} = \frac{\pi}{\beta_0 - \beta_1} \approx \frac{4n_r W_e^2}{3\lambda} \quad (12)$$

The effective width can be given as

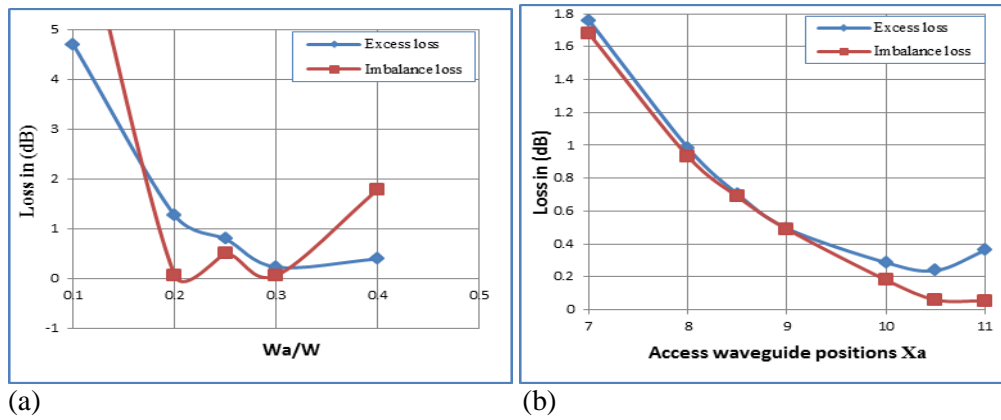
$$W_e \approx W + \frac{\lambda}{\pi} \left(\frac{n_e}{n_r} \right)^{2\sigma} / \sqrt{n_r^2 - n_c^2} \quad (13)$$

Where

(W) is the physical width of the MMI area, (n_r) and (n_c) are the effective core index and the effective cladding index, respectively, λ is the free-space wavelength and the integer (σ) = 0 for the (TE) modes and (σ) = 1 for the (TM) modes [11,12].

The silica material which is used to design the coupler has core refractive index (n_r) equal to 1.47. Typically the core diameter of a single mode fiber has a value ranging from 8 to 10 μm , the access waveguide width for the coupler (W_a) is 9 μm to be compatible with the single-mode fiber. According to equation ($W_a < \frac{2.4 \cdot \lambda}{\pi \cdot \text{NA}}$) the numerical aperture (NA) must be less than 12.15% therefore, the cladding refractive index n_c was chosen to be 1.465 [13].

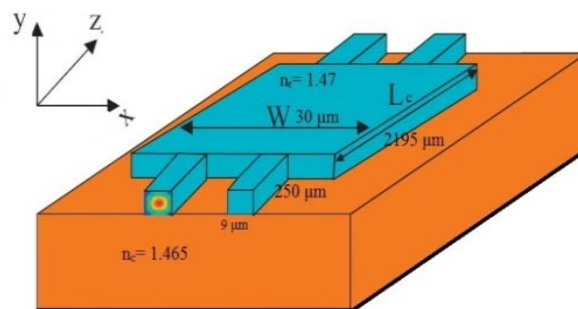
The excess loss and the imbalance are important characteristics of a 3dB MMI coupler which depend on the coupler geometry. Fig. 2 (a) shows the characteristic of the 3dB MMI coupler for various physical width of the MMI area. From Fig. 2(a) it can be noted the excess loss and the imbalance loss of the coupler are minimum at $W_a/W=0.3$, the W is defined as a physical width of the MMI area of the coupler, which is 30 μm . The effective thickness (h) is equal to 9 μm and the coupler length (L_{MMI}) for 3dB coupler is equal to 2195 μm . The optimization of the 2x2 3dB MMI coupler which comprises a fine-tuning of the MMI coupler geometry of low excess and imbalance losses. After the value of the MMI coupler physical width (W) and the access waveguide width (W_a), we can calculate the value of the access waveguide positions (X_a). Fig. 2 (b) shows the excess and the imbalance losses variation at different access waveguide positions. Fig.3 shows the 3D structure of the 3dB MMI coupler. Table (1) shows the design parameters of the 3dB MMI coupler. The finite difference beam propagating method (BPM) is used to design and simulate of the 3dB MMI coupler, Fig.4. shows the optical field propagation of the 3dB MMI coupler.



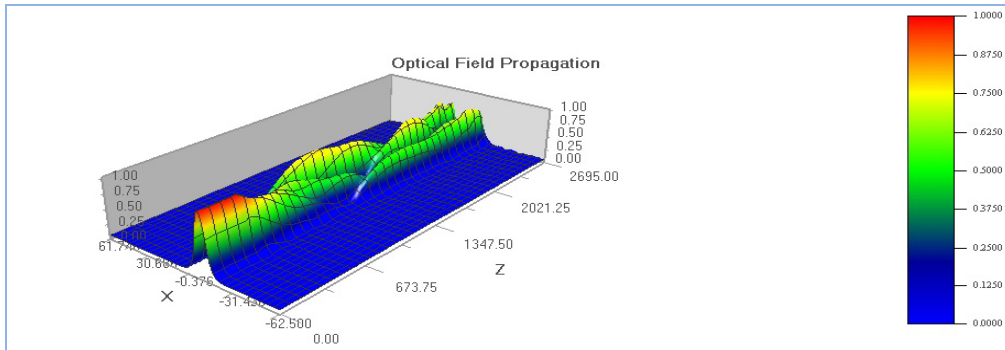
Figure(2). The change in the characteristic of the 3dB MMI coupler. (a) The variation in the excess loss and the imbalance with physical width of the MMI area (W). (b) The variation in the excess loss and the imbalance with the access waveguide positions (X_a)

Table (1) The design parameters of the 3dB MMI coupler

Parameters	Dimension
W_a	9 μm
W	30 μm
W_e	34 μm
L_{MMI}	2195 μm
X_a	10.5 μm
Taper length (L_{tap})	250 μm
Thickness (h)	9 μm

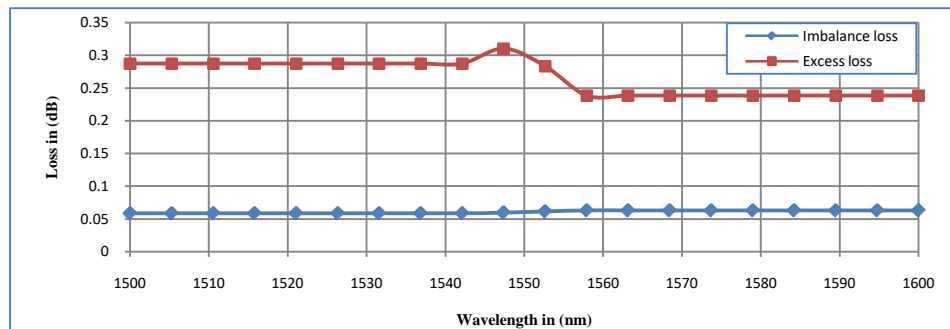


Figure(3).The 3D structure of the 3dB MMI coupler



Figure(4). The optical field propagation of the 3dB MMI coupler

The achievable bandwidth of 2×2 3dB MMI couplers is determined by wavelength dependent calculations. In this research excess and imbalance losses as a function of wavelength had been studied as shown in Fig.5. The excess loss of the 2×2 3dB MMI coupler never exceeds 0.28 dB over the band (1500 nm -1600 nm) and the imbalance loss never exceeds 0.064 dB. The excess loss is 0.23 dB and the imbalance loss is 0.06 dB at a wavelength equal to 1550 nm and power of 1mw (0 dBm).



Figure(5). Excess loss and imbalance loss as a function of wavelength

The design of the Bragg grating

A Bragg grating is a permanent periodic modulation of the refractive index along a given length of the optical waveguide, formed by utilizing the photosensitivity of germanium-doped silica glass. The first order Bragg condition is simplified as.

$$\lambda_B = 2 n_{eff} \Lambda \quad (14)$$

The Bragg grating wavelength (λ_B) is the free space wavelength of the input light that will be reflected back from the Bragg grating, (n_{eff}) is the effective refractive index of the fiber core and (Λ) is the grating spacing of the BG.

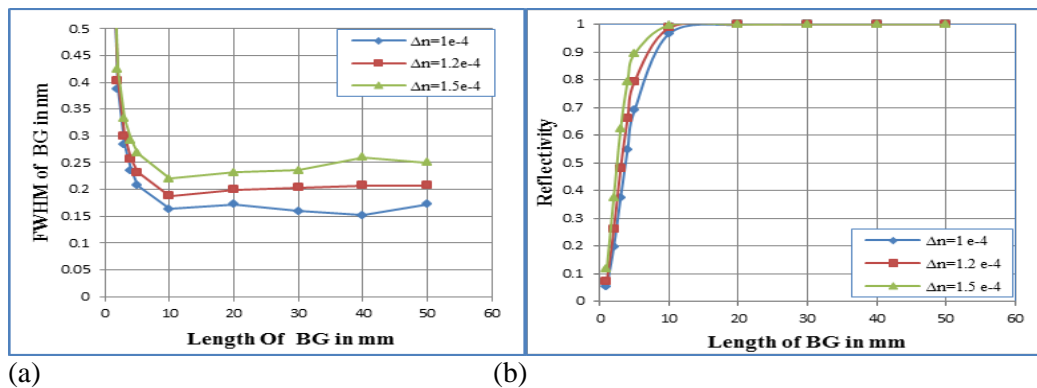
A grating can be represented by the formula that combines a grating shape function, an average index modulation function, a period chirp function, and the apodization function. The effective refractive index (n_{eff}) can be written as follows:

$$n_{eff}(x,y,z) = n_r(x,y) + \Delta n_r(x,y,z) + \Delta n \cdot P(x,y) \cdot A(z) \cdot f[\Lambda(z)/\cos\theta, z] \quad (15)$$

Where:

n_r is the waveguide refractive index, Δn is the index modulation amplitude, θ is the grating tilt angle, $f[\Lambda(z)/\cos\theta, z]$ is the shape function, Δn_r is the average index modulation function, $\Lambda(z)$ is the period chirp function, $A(z)$ is the apodization function and P is the photosensitivity profile of waveguide [15].

In Eq. (15), the average index modulation function Δn_r is applied only in the region of the grating, in the layers with non-zero photosensitivity. Layers with very small photosensitivity will respond to the average index modulation, but the grating will be very weak there. To calculate the optimum value of the BG length and index modulation amplitude of the BG, the maximum value of Δn equal to 4×10^{-4} in order to the FWHM bandwidth for the FBG equal to 0.208 nm (25 GHz). In the design the (Δn) must be less than the maximum value in order to obtain a suitable length of the BG. Typically the index modulation amplitude (Δn) ranges from (10^{-3} to 10^{-5}). In WDM communication system BG length and (Δn) must be adjusted to optimize BG characteristics, including FWHM bandwidth and maximum power reflectivity. Fig. 6.(a) shows different values of the FWHM bandwidth as a function of BG length at different values of the index modulation amplitude (1×10^{-4} , 1.2×10^{-4} , 1.5×10^{-4}). For a given value Δn the FWHM bandwidth decreases with an increase in the BG length to a constant value. The constant value can be increased or decreased by increasing or decreasing the value of Δn .



Figure(6).(a) The variation in the FWHM bandwidth as a function of BG length. (b) The variation in reflectivity with the BG length.

Fig. 6(b) shows the change in the reflectivity with the change of the BG length at different values of Δn (1×10^{-4} , 1.2×10^{-4} , 1.5×10^{-4}), the figure shows that maximum power reflectivity is increased with the increase in the BG length towards 100% reflectivity. This variation can be accelerated by increasing (Δn) . Several modifications are required in the setting dialog box to change the values of index modulation amplitude (Δn) and the BG length (L_g) can be obtained from Fig. (6 (a), 6 (b)). The length (L_g) was found to be equal to 50 mm at index modulation amplitude (Δn) of 1.2×10^{-4} . The basic parameters of uniform BG, is shown in Table (2).

Table (2) The parameters of the designed BG

Parameters	Sitting	Parameters	Sitting
Grating shape	Rectangular	Waveguide thickness	9 μm
Average index	Uniform	Core index	1.47
Period chirp	No chirp	Cladding index	1.465
Apodization	No apodization	Grating period	0.52762870 μm
Length (L_g)	50 mm	Waveguide width	9 μm
Index modulation amplitude (Δn)	0.00012		

Simulation

The optical transmission link consists of four main elements which they are the transmitter, Optical transmission channel, the OADM and the receiver as shown in Fig. 7.

The OADM has four parts, namely input port, add port, drop port and output port. Sixteen channels (Tx) with start center frequencies 194.216 THz (1543.6 nm) and the space between channel 100 GHz (0.8 nm) are fed to the input ports. A channel with frequency 193.4144 THz (1550 nm) is dropped and the same frequency is added from the add port. Each transmitter is composed of data source, NRZ rectangular driver, laser source, optical amplitude modulator. Data source generates a binary sequence of the data stream and the source is customized by baud rate, sequence and logical. The model has sixteen center emission frequencies, 1 mW (0 dBm) CW power, laser noise bandwidth equal to the sample rate and 10MHz FWHM line width with 10 Gbps bit rate. The OADM has a filter of bandwidth equal to 25 GHz (0.208nm), and add/drop frequency of 193.4144 THz (1550 nm). In the receiver a PIN photodiode has a responsivity equal to 1 A/W, dark current equal to 10 nA, approximate sensitivity -18 dBm and low-pass Bessel filter with cut frequency equal to $0.6 \times \text{Bit rate}$. The optical transmission channel consists of single mode fiber (SMF-28), dispersion compensating fiber (DCF) and Erbium Doped Fiber Amplifier (EDFA), Table (3) shows the main characteristic of the optical transmission channel components is used in simulation.

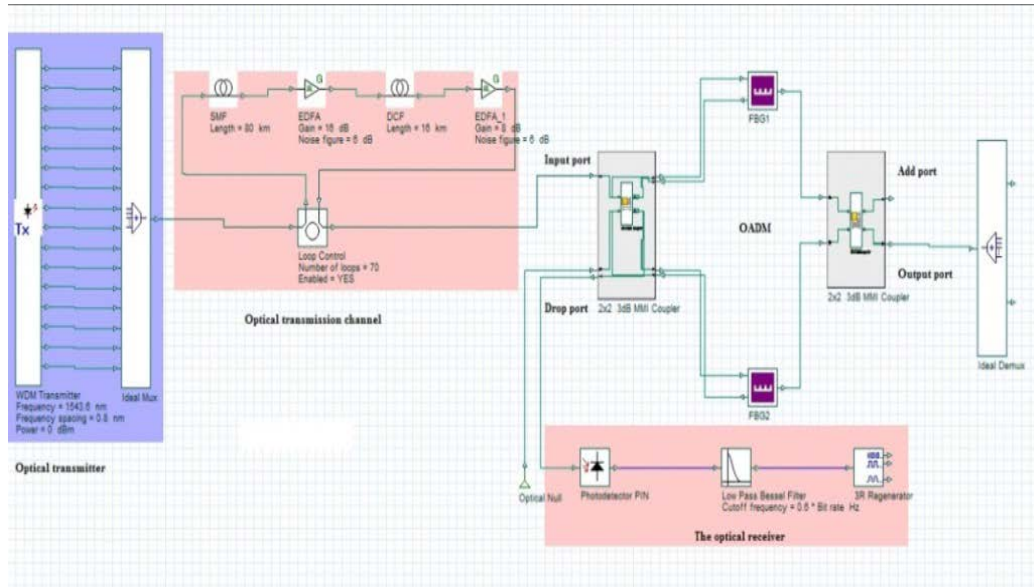


Figure (7). Optical transmission link

Table (3) The main characteristic of the optical transmission channel components

SSMF-28 main parameters		DCF	
The parameter	Setting	The parameter	Setting
Length	80 Km	Length	16 km
Attenuation	0.185 dB/km @1550 nm	Max Attenuation	0.5 dB @ 1400 nm
Dispersion	16.5 ps/nm/km @1550 nm	Effective area (A_{eff})	32 μm^2 @ 1550 nm
Nonlinear index of refraction	$2.6 \times 10^{-20} m^2/w$	Dispersion	-82 ps/nm/km @ 1550 nm
Effective area (A_{eff})	76.5 μm^2 @ 1550		
EDFA -1		EDFA -2	
Optical fiber amplifier type	EDFA	Optical fiber amplifier type	EDFA
Gain	16 dB	Gain	8 dB
Noise figure	6 dB	Noise figure	6 dB

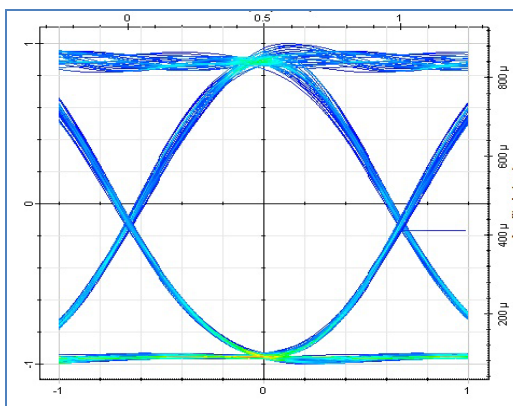
Results and discussion

The performance of OADM component was studied using a broadband signal around 1550 nm. The wavelength of the dropped signal =1550 nm, this represents the worst case of the system because of the dropping signal at the center of the band. The NRZ modulation format was chosen to be (NRZ) because it is widely used in optical communication systems. The performances of the OADM results are shown in Table (4) when sixteen channels are used in DWDM systems.

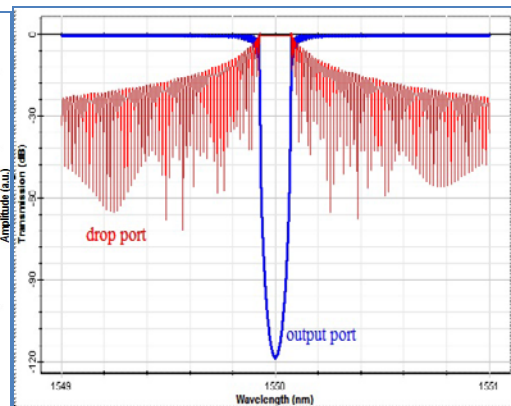
Table (4) performance results of the OADM

Item Description	Value	Item Description	Value
Channel Spacing	100 GHz (0.8 nm)	Bit rate	10 Gb/s
Wavelengths operation	(1543.6 -1556.4) nm	Q – factor	62.5
Pass band @ 0.5dB	0.156 nm (19.39 GHz)	Operation Temperature	-20 to 60 °C
Band pass filter bandwidth @ (3dB)	0.208 nm (25 GHz)	Fiber type	SMF-28
Band pass uniformity bandwidth @ (3dB)	≈ 0 dB		
Insertion loss	0.6 dB		
The intraband crosstalk	< -49 dB		
The interband crosstalk (adjacent channel)	< -28 dB		
Non-adjacent channel isolation	> 55 dB		
Return loss	> 55 dB		
Isolation between add and drop	> 80 dB		
Polarization dependent loss (PDL)	0.00446 dB		
Polarization dependent wavelength shift (PDW)	0.004 nm		
Optical power handling range	10 dBm to -10 dBm		

Fig.8. shows a clean opening - eye diagram pattern when 1550 nm signal is dropped, it is observed from the eye pattern that the vertical eye opening is equal to 747.187 μ a.u (Max eye opening factor is 98.4 %). This means intersymbol interference (ISI) and noise is very low. Fig.9. shows the transition function of the OADM when 1550 is a dropped signal and when a band pass filter is used with center frequency of 1550 nm and FWHM bandwidth equal to 0.208 nm.

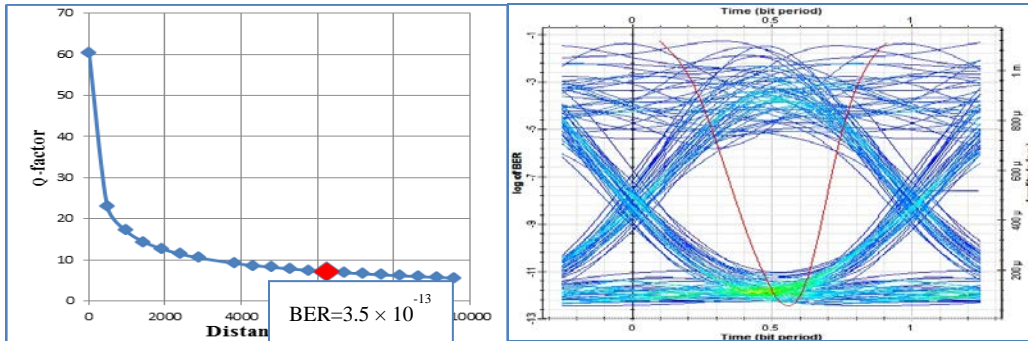


Figure(8). The eye diagram of the digital signal when 1550 nm signal is dropped



Figure(9). The transition function of the OADM when 1550 is a dropped signal

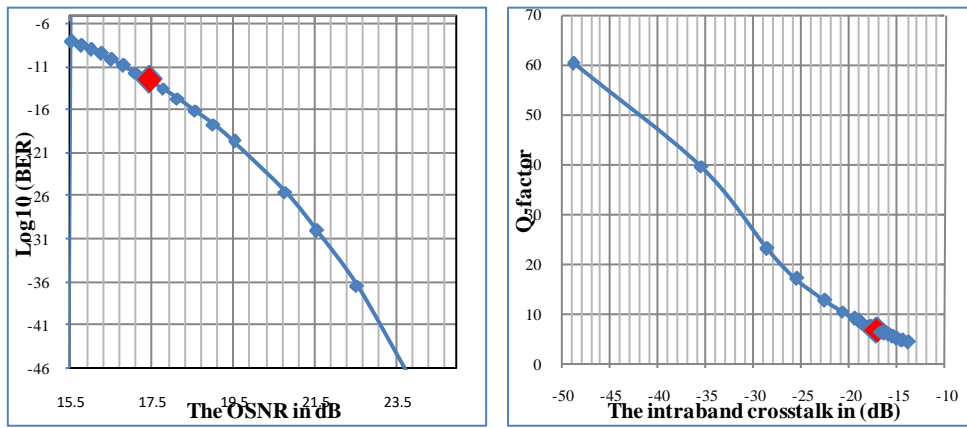
The variation between the Q-factor and fiber transmission distances is shown in Fig.10, it indicates that the system can detect the dropped signal (1550 nm) when the fiber transmission distances is equal to 6250 Km. At this distance the Q-factor is equal to (7.15), the OSNR is equal to (17.5 dB) and the BER is (3.5×10^{-13}). Fig.11 shows the eye pattern when the fiber transmission distances at 6250 km.



Figure(10). The variation between Q-factor coverage distance

Figure(11). The eye pattern at 6250 km

Fig.12. (a) shows the BER as a function of the OSNR (for the 1550 nm dropping signal), at the distance range is from 1440 km to 9600 km. It can be observed the OSNR is decreased by 2dB, when the distance increased from 6250 km to 9600 km. Fig.12. (b) shows the Q-factor with intraband crosstalk (for the 1550 nm dropping signal), it can be observed the Q-factor has decreased with increased the intraband crosstalk. The figure shows the system can detect the dropped signal (1550 nm) when the intraband crosstalk is less than -17.5 dB.



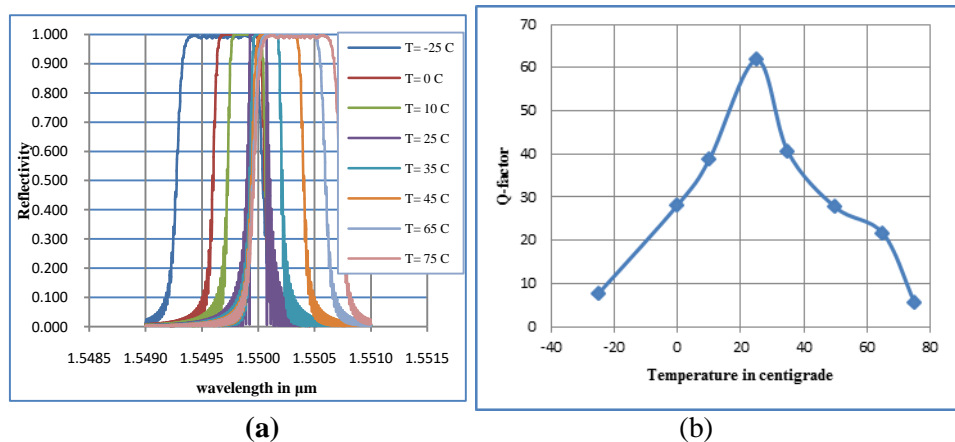
(a) (b)
Figure(12) (a) The BER as a function of OSNR.(b) The Q-factor with intraband Crosstalk

Temperature Sensitivity

In the optical communication, working temperature is one of the important effects on WDM components and the BGs design. The change in the grating period (Λ) of the BGs due to variation of temperature is a major factor in the shifting of the central wavelength of a channel. To study the working temperature effect on the performance of OADM system a linear temperature coefficient was chosen to be $(0.013717 \text{ nm} / ^\circ\text{C})$. Fig.13.(a) shows the reflection power spectrum of the BG at different temperatures, the shift in the resonance wavelength with strain and temperature can be expressed using [15].

$$\Delta\lambda_B = \lambda_B (K_T * \Delta T + K_\epsilon * \Delta\epsilon) \quad (16)$$

Where ΔT and $\Delta\epsilon$ are the changes in temperature and strain, respectively, and the coefficients K_T and K_ϵ are the temperature and strain sensitivities of the resonance wavelength shift ($\Delta\lambda_B$), respectively. The change in Q-factor at different temperatures is shown Fig.13. (b). From this figure, it can be observed that the system performance is reduced in temperature different from the specific temperature at which the system is designed (in our design specific temperature = 25°). In the DWDM system the shifting of the central wavelength is not accepted because the DWDM system works at narrow guard bandwidth. In order to reduce the temperature effect a low thermal expansion material must be used or a temperature control system to keep the system at stable temperature



Figure(13). (a) The reflection power spectrum of the BG at different temperatures.(b) The change in Q-factor at different temperatures

Conclusion

From the performance of the proposed OADM which was studied and from the simulation results the following conclusions are drawn.

Crosstalk depends on the reflectivity and bandwidth of the BGS. When the reflectivity increases the crosstalk decreases and when the BGs bandwidth is increased the crosstalk is also increasing, the best performance of the crosstalk is when the BGS bandwidth is equal to 25% of the space channels in the DWDM system.

The bandwidths of -3dB and -20dB are 0.208 nm (25 GHz) and 1.46 nm (180 GHz) respectively, when 1550 nm is used as dropped signal, hence it's suitable for 100 GHz space channel applications. The -3dB bandwidth of the BG filter can be made narrower while keeping the same grating strength by increasing length of the BG (L_g) or decreasing the index modulation amplitude (Δn) for the lower space channel applications.

The proposed design of the OADM has many advantages such as reducing insertion loss, reducing size and cost, because this system does not need any circulators or isolators. The circulators or isolators are replaced by using two 3dB MMI couplers. The OADM design consists of the BG and MMI coupler which can be made by the planar Lightwave circuit (PLC) technology.

The proposed OADM can be connected in cascaded form to designed N-channels of MUX/DEMUX where the insertion loss has increased with the increasing of number channels, but this technique improves the crosstalk of the system.

REFERENCES

- [1]. Martin T. Hill et al, "Optimizing Imbalance and Loss in 2X2 3-dB Multimode Interference Couplers Via Access Waveguide Width," *J. of Lightwave Technology* **21**(10), 2305-2313,(2003).
- [2]. Filho A.F.G.F. et al, "A Performance Study of a Nonlinear all Fiber Michelson Interferometer, Add-Drop Multiplexer, Based in Fiber Bragg grating Mirrors," *J. Opt Quant Electron* (40), 525-534, (2008).
- [3]. Hongqiang Li et al, "Highly Compact 2x2 Multimode Interference Coupler in Silicon Photonic Nanowires for Array Waveguide Grating Demodulation Integration Microsystem," *J. Optics & Laser Technology* (47), 366-371 ,(2013).
- [4]. Sumei Wu, Xingdao He and Chenbo Shen, "Design and Fabrication of Multimode Interference Couplers Based on Digital Micro-Mirror System," *SPIE* **6832** (68321Z-1), (2008).
- [5]. Huiye Qiu et al, "Silicon mode multi/demultiplexer based on multimode grating-assisted couplers," *Opt. Express* **21**(15),17904-17911,(2013).
- [6]. Soldano L. B., and Pennings C. M., "Optical Multimode Interference Devices Based on Self-Imaging Principles and Applications," *J. Lightwave Technology* **13** (4), 615-627, (1995).
- [7]. Kazimir Y. Kolossovski, Rowland A. Sammut, "Three-step design optimization for multi-channel fibre Bragg gratings," *Opt. Express* **11**(9) ,1029-1038, (2003).
- [8]. Turan Erdogan, "Fiber Grating Spectra," *J. of Lightwave Technology* **15**(8),1277-1294, (1997).
- [9]. Rongqing Hui, Maurice O'Sullivan, "Fiber Optic Measurement Techniques," Elsevier Inc, San Diego, 2009.

- [10]. Raman Kashyap, "Fiber Bragg Gratings," (Academic Press, San Diego, 1999).
- [11]. Masaaki IMAI and Shinya SATO, "Optical Switching Devices Using Nonlinear Fiber-Optic Grating Coupler," *Photonics Based on Wavelength Integration and Manipulation*, 293–302, (2005).
- [12]. Cheng-Ling Lee, Ray-Kuang Lee and Yee-Mou Kao, "Design of Multichannel DWDM Fiber Bragg Grating Filters by Lagrange Multiplier Constrained Optimization", *Optics Express* **14** (23), 11002-11011, (2006).
- [13]. Xiao-Jun Wang, Wei-Wei Ke and Hua Su1 "Thermal-induced two dimensional beam distortion in planar waveguide amplifiers," *Opt. Express* **21**(15) , 17999-18010, (2013).
- [14]. Mohammad Syuhaimi Ab-Rahman et al, "Optical System Monitoring Based on Reflection Spectrum of Fiber Bragg Grating," *J. of Computer Science* **8** (6), 1001-1007, (2012).
- [15]. S. T. Oh, W. T. Han, U. C. Paek, and Y. Chung, "Discrimination of temperature and strain with a single FBG based on the birefringence effect," *Opt. Express* **12**(4) , 724-729 (2004).